Group Studies Worksheet

Sharif Khan-Bennett

SXK1015

February 2020

1 General Asteroseismology.

I have reordered the questions a little for a smoother narrative.

1.1 Granulation.

The Schwarzschild criterion states that a bubble of gas will rise if it is lighter than the surrounding material and sink if it is heavier. By treating the plasma of a star like an ideal gas, a bubble will experience buoyant forces, these are found by considering its temperature compared to the temperature gradient of the surrounding plasma. If the adiabatic gradient in a star is smaller (less negatively steep) than the ambient temperature gradient, a hot bubble of gas won't lose energy quick enough as it rises to reach equilibrium because of a growing excess of heat compared to its surroundings. It will rise until the density of the surrounding material drops off enough such that the buoyant force reaches equilibrium with its weight. This is the process that causes convection in stars.

Since the net upward and downward motion must be equal, the convective flux must be constant throughout the star. Nearer to the surface of the star, at the edge of the convective zone, the opacity is much smaller because of the density and temperature dropping off, allowing energy to be lost via radiation. Therefore, to keep the convective flux constant at the surface, the temperature gradient must become steeper. This happens so much that the difference between the ambient temperature gradient and the adiabatic gradient grows so large that the region is superadiabatic. A rising bubble will accelerate through this region such that it overshoots the photosphere resulting in a hot, bright cell to be seen on the surface of the star. It then radiates energy and cools down, causing the density to increase followed by it sinking back down to the convection zone. The overshooting and subsequent sinking results in oscillatory motion at the surface of the star where hotter brighter regions rise until they cool, darken and fall back down. This mechanism manifests in a granulation pattern at the surface of the star.

These convective cells have typical diameters of 1000 km and oscillate at relatively low frequencies, approx 110µHz. These cells appear across the entire surface of the star and are the driving mechanism for standing

waves found within the star.

1.2 The amplitudes and damping rates of the modes.

Due to the granulation being inherently random, they simultaneously excite and damp the standing waves. An illustrative analogy would be to think of a bell, representing the star, in a sandstorm where some grains of sand, representing the convective cells, impact in such a way that it drives a net oscillation and subsequent ringing whereas others damp and reduce the ringing of the bell. Since the resonant driving frequencies and the stellar parameters only allow certain frequencies to oscillate through the star's interior, a Gaussian distribution of frequencies are set up and will be discussed in later questions. Each damped oscillation on the power frequency spectrum is Lorentzian in shape, exhibiting a lot of fluctuation about the Lorentzian fit due to the random nature of the driving force. The damping rate $\pi\tau^{-1}$ is found from the FWHM, where τ is the timescale associated with the damping constant. The amplitude of the mode is set from the balance between excitation and damping from the granulation. The surface gravity determines the height of the Lorentzian where a smaller surface gravity results in a greater amplitude of the Lorentzian.

1.3 P-modes.

P-modes are the standing waves that are set up because of coherent excitations from convective cells at the surface of the star. They are projected into the stellar interior at a range of angles and experience refraction back towards the surface as a result of the temperature gradient within the star. As a result, only the modes with no angular component (ones that are projected tangential to the stellar surface) reach the core of the star. The "p" refers to the fact that the restoring force is the pressure gradient within the star. Due to the damping from the granulation, their power spectra resemble a Lorentzian. There is a range of modes that oscillate through the star's interior depending on the internal properties of the star. Each mode is assigned a radial order, n, and angular degree, l, as a result of the way the mode distorts the shape of the star where radial modes have $l = 0$. Because of geometric cancellation and technical limitations, it is difficult to observe angular degrees greater than $l = 2$. Geometric cancellation refers to the symmetry of modes on either side of a star causing difficulty in measuring changes in its observed flux.

The following equation gives the positions of the p-modes on the frequency spectrum

$$\nu_{n,l} \simeq \Delta\nu\big(n + \frac{l}{2} + \epsilon\big) - Dl(l+1). \tag{1}$$

$\Delta\nu$, D and ϵ are related to the average density, the sound speed gradient and the surface conditions, they are discussed in the following sections.

1.4 The large frequency separation, $\Delta\nu$, of p-modes.

The large frequency separation is the separation between corresponding angular degrees in adjacent radial orders, it is given by $\nu_{n+1,l} - \nu_{n,l} \simeq \Delta\nu$. The angular degrees within each radial order follow a regular, repeating pattern. Dividing the spectrum into segments of width equal to $\Delta\nu$ and stacking the segments on top of each other form an echelle diagram, displaying straight lines which represent each observed angular degree. Deviation from a straight line indicates that an incorrect spacing has been used.

The observed large frequency separation scales to a good approximation to the square root of the average stellar density. Therefore, as a star gets older and its density decreases, the large frequency separation gets smaller and the observed Gaussian of p-modes gets narrower.

Epsilon from equation 1 is determined by the cavity boundary conditions of the star, in particular, the effective temperature of the star. It has the effect of changing the frequency of the modes by factors of the large-scale separation. This can be understood using a wave trapped in a pipe with one open end at the surface where the "openness" of the pipe at the surface is set by the acoustic cut-off frequency as defined in the next section. Epsilon usually takes values between 1 and 2.

$$\Delta\nu \simeq < \rho >^{\frac{1}{2}} \propto \left(\frac{M}{R^3}\right)^{\frac{1}{2}} \tag{2}$$

1.5 The small frequency separation, $\delta\nu_{02}$, of p-modes.

The differences in frequency of modes with different l result from them being projected into the stellar interior at different angles. This causes them to reach different depths within the star before the star refracts them towards the surface, causing small changes in the observed frequency for each angular degree. Wave modes with a smaller l penetrate more deeply into the star. As a result, these modes are used to probe the conditions such as the hydrogen mass fraction in the stellar core which can indicate its age.

The small frequency separation is the difference in frequency between two angular degrees within the same n, $\delta\nu_{n,l} = \nu_{n,l+1} - \nu_{n,l}$. D scales all the small frequency separations as $Dl(l+1)$, resulting in $\delta\nu_{01} = 2D$, $\delta\nu_{02} = 6D$, $\delta\nu_{13} = 10D$ etc. These also correspond to the separations between the corresponding vertical lines on the echelle diagram. D depends on the sound speed gradient in the star's interior, it is given by

$$D = \left(4\pi^2\Delta\nu\right)^{-1}\left[\frac{c(R)}{R} - \int_0^R \frac{dc}{dr}\frac{dr}{r}\right]. \tag{3}$$

1.6 The frequency of maximum oscillations power, ν_{max}, of the p-modes.

As described in the amplitude and damping section, there is a range of excitation frequencies which drive the p-modes. These frequencies follow a Gaussian distribution, which forms the envelope that scales the Lorentzians. There is a frequency which produces the largest power at the peak of the Gaussian. This

parameter carries information about the surface conditions of the star and relate to the cut-off frequency, as given by

$$\nu_{ac} = \frac{c}{2H} \tag{4}$$

where H is the density scale height.

There is a sharp rise in ν_{ac} close to the surface of the star which acts as the effective reflecting surface for the standing wave, this fixes the maximum frequency, ν_{max} of standing waves which can be contained within the star. The sun has a maximum frequency of oscillation of 3.05mHz [1]. As stars evolve, the surface gravity decreases, causing ν_{max} to decrease, shifting the Gaussian envelop to lower frequencies.

$$\nu_{max} \propto \nu_{ac} \propto \frac{c}{H} \propto g T_{eff}^{-\frac{1}{2}} \tag{5}$$

2 Stellar populations.

2.1 CMD and HR diagrams.

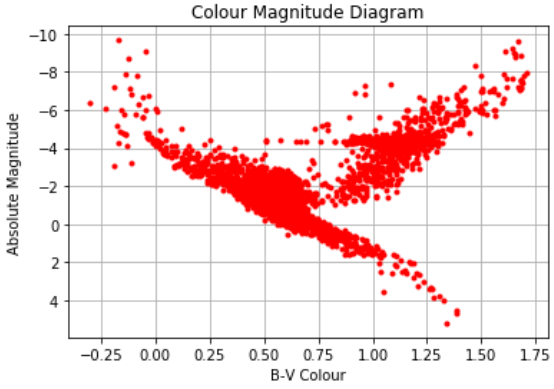

(a) Colour Magnitude diagram for the stars in the synthetic data

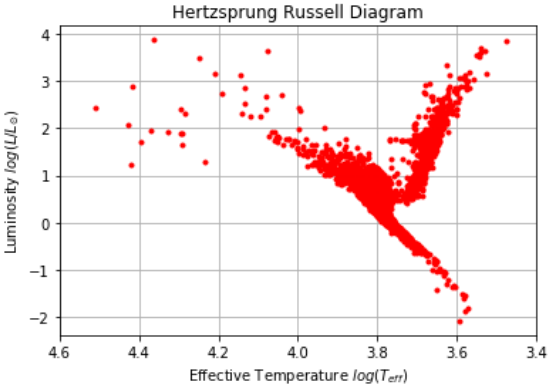

(b) Hertzsprung Russell diagram for the stars in the synthetic data. Note that one point had been removed which lie at $T_{eff} > 5.0$. This was done to investigate the bulk of the stars at lower temperatures in greater detail.

2.2 Description.

2.2.1 2i

The absolute magnitude along the y-axis relates to the luminosity via the logarithm equation. This relates the difference in the absolute magnitude of the star in question with that of the sun with the ratio of their

luminosities as given by the following equation

$$M_{star} - M_{\odot} = -2.5log_{10}\left(\frac{L_{star}}{L_{\odot}}\right). \tag{6}$$

The B-V colour index is the difference in absolute magnitudes measured through the B and the V filter. Like temperature, this is a measure of the energy of the emitted photons. Since the B-band is transparent to higher energy photons than the V-band, a higher T_{eff} results in the B-band magnitude being more negative than the V-band magnitude, hence the (B-V) index being more negative in total. They are related by the following equation

$$T_{eff} = 4600K\left(\frac{1}{0.92(B-V)+1.7} + \frac{1}{0.92(B-V)+0.62}\right).[2] \tag{7}$$

If the plot used apparent magnitude instead of absolute magnitude, it would display a more random arrangement of points along the y-axis. This is caused by the apparent magnitude being affected by the distance of objects unlike in the case of the absolute magnitude. Since all the stars in the catalogue are not necessarily at the same distance, the apparent magnitude with vary greatly from star to star as a result of varying distances from Earth. There will be a maximum cut-off magnitude relating to the sensitivity of the telescope this was found to be at $14mag$. The distribution along the x-axis will remain unchanged.

2.2.2 2ii

The Hertzsprung–Russell diagram displays two distinct regions, the downward sloping main sequence branch, where stars spend most of their lifetimes, fusing hydrogen into helium and the upwards sloping red giant branch, where helium-fusing stars are plotted. It could be inferred that the simulation represents an old population of stars since there appear to be fewer stars at temperatures greater than log(4.2)K, and a large proportion of stars past the main sequence turn-off point and in the red giant branch. There are also few stars at luminosities less than $10^{-1}L\odot$, the low mass end of the diagram. If these data points had been measured with a telescope (as opposed to being simulated), it could indicate the lack of sensitivity of the telescope in being able to detect dim objects. This is where smaller objects lie, including white dwarfs at higher temperatures, and red dwarfs at lower temperatures, in line with the main sequence stars. As these red dwarfs are the subject of this group studies project, I would suggest that we should not use this hypothetical telescope.

The density of points in this plot indicates the time that stars spend in each evolutionary phase. As already suggested, the absence of stars in the top left corner of the Hertzsprung–Russell diagram shows that large, hot stars have relatively short lifetimes and that the plotted population is older than this. There is also a drop in density at the turn-off point, this is known as the Hertzsprung–Russell gap. It indicates that stars which have exhausted their hydrogen evolve much quicker into red giants than they do through the main sequence and red giant phases separately. This is also represented on the colour-magnitude diagram at B-V colour $\simeq 0.75$.

The colour-magnitude diagram has very similar features to the Hertzsprung–Russell diagram since they are essentially only re-scaled plots. The turn-off point can be seen on the colour-magnitude diagram at B-V $\simeq 0.75$ which connects the upward-sloping red giant branch to the downward sloping main sequence branch. More generally, Hertzsprung–Russell diagrams which include stars from clusters of a range of ages would include the short-lived blue giants at the top left of the plot, red supergiants above the red giant branch, and the main sequence stars, red giants and the white and brown dwarfs already mentioned.

3 Quantitative Asteroseismology.

3.1 Plotting $\Delta\nu$ and $\delta\nu_{02}$ as a function of frequency.

The plots of the $\Delta\nu$ as a function of ν for each star as seen in figure 2 have similarities and differences. They all display the large separation initially falling and then rising at higher frequencies. This could be as a result of ϵ increasing with frequency or due to other higher-order effects. They also display that modes with greater l have a greater $\Delta\nu$, indicating that ϵ could be bigger for greater values of l. Since the $\Delta\nu$ of each angular degree moves in unison, any $\Delta\nu_{n,l}$ is a good approximation of $\Delta\nu$.

The plots differ in the fact that the plots representing the older stars have p-modes defined over a range of smaller frequencies, caused by ν_{max} being smaller for larger stars because of a smaller surface gravity, g and effective temperature, T_{eff}. Older stars also have smaller $\Delta\nu$ as explained in the next question.

The final plot shows how the small separation between the $l = 0$ and $l = 2$ modes vary as a function of frequency. Older stars have a smaller $\delta\nu_{02}$, as explained in the next section. It also appears that the small separation shrinks for greater values of n and at increased rates for older stars, represented by the downward slopes for each star. This could be because of higher-order effects on D.

3.2 How $\Delta\nu$ and $\delta\nu_{02}$ evolves as a function of time.

To plot the average large separation against the central hydrogen mass fraction, the average $\Delta\nu$ was taken across all radial modes and all angular degrees. To plot the small separation, the average separation between the $l = 0$ and $l = 2$ across all radial modes were considered. It can be seen from the plots at older stars have a smaller central hydrogen mass fraction and have a smaller average $\Delta\nu$ and $\delta\nu$. By plotting the average $\delta\nu$ against the average $\Delta\nu$, a Christensen-Dalsgaard diagram is produced which shows this, as seen in figure 3.

Older stars have a smaller $\delta\nu$ due to them having a smaller value for D. This parameter depends on the sound speed gradient which is dependent on the metallicity and mass fraction of the core. Therefore, since older stars have a smaller proportion of hydrogen; they can be expected to have smaller values of D. They also have a smaller $\Delta\nu$ since this parameter is proportional to the square root of the average density which shrinks with time as the star expands.

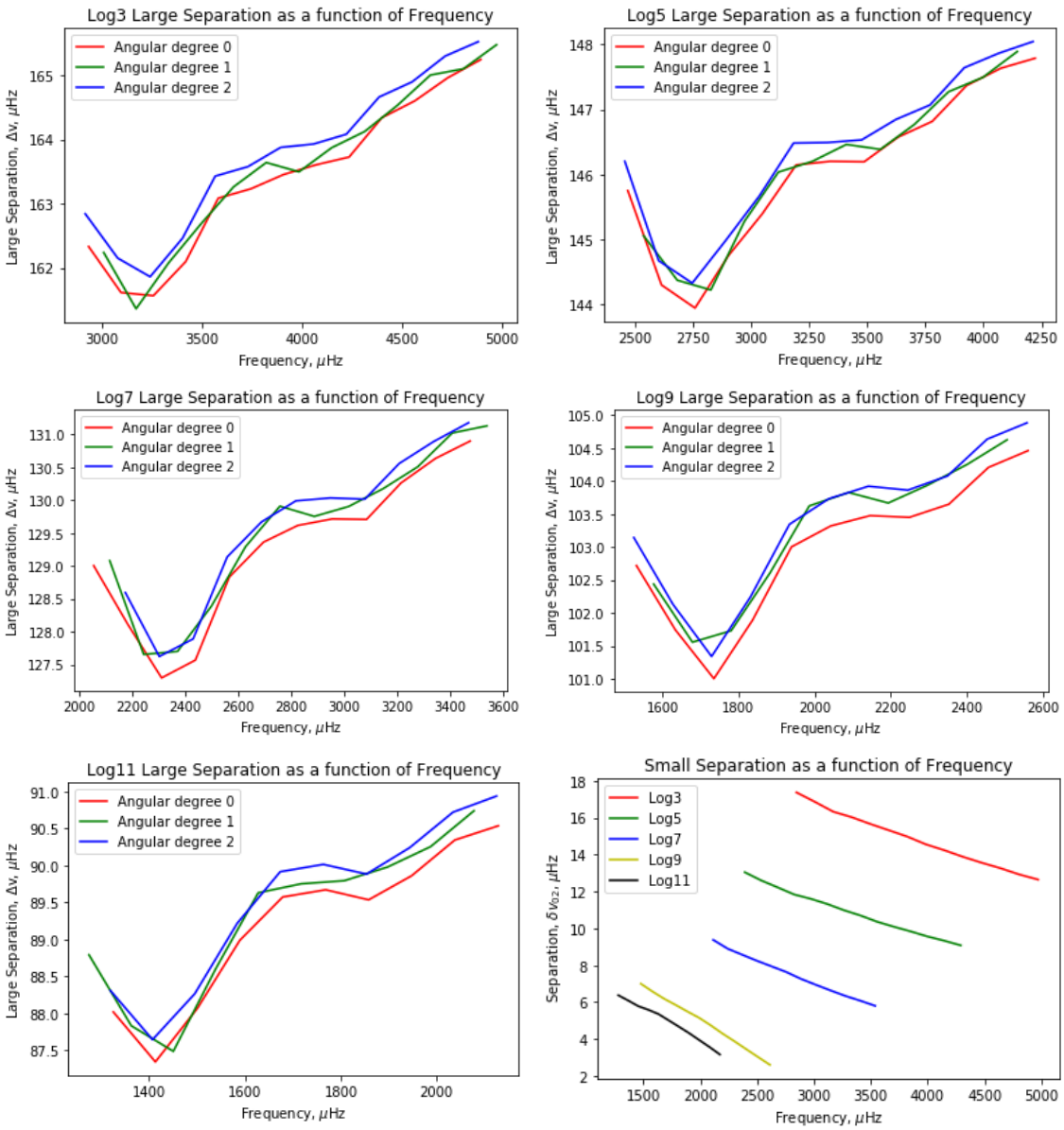

Figure 2: $\Delta\nu$ for the 5 stars measured individually between the $l = 0, 1, 2$ modes. The bottom right figure is a plot of $\delta\nu_{02}$ as a function of frequency for the 5 stars.

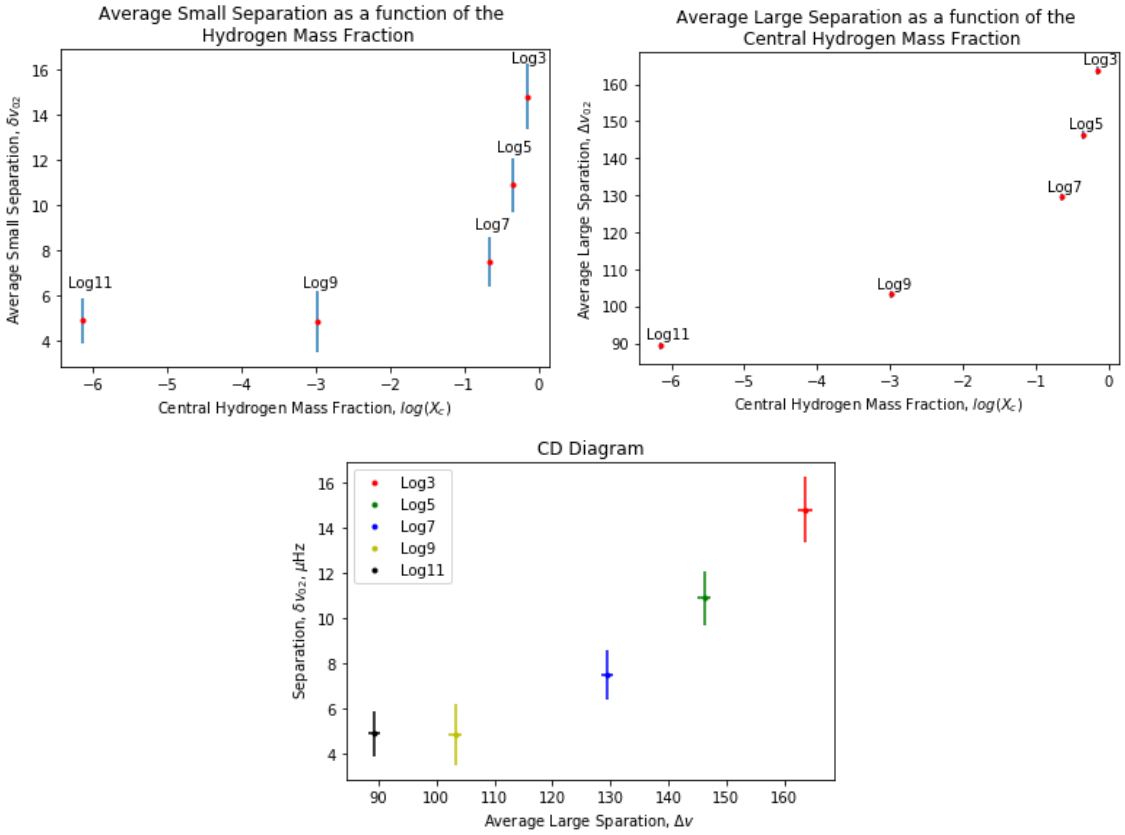

Figure 3: How the $\Delta\nu$ and $\delta\nu$ change as a function of the log of the Hydrogen mass fraction. The bottom figure plots the y-axis of the top left figure against the y-axis of the top right figure to obtain a Christensen-Dalsgaard diagram.

References

[1] H Kjeldsen and TR Bedding. Amplitudes of stellar oscillations: the implications for asteroseismology. *arXiv preprint astro-ph/9403015*, 1994.

[2] FJ Ballesteros. New insights into black bodies. *EPL (Europhysics Letters)*, 97(3):34008, 2012.